Research Article

Farah M. Al-Askar*

Optical solitons to the fractional Kundu–Mukherjee–Naskar equation with time-dependent coefficients

https://doi.org/10.1515/phys-2024-0102
received May 14, 2024; accepted November 14, 2024

Abstract: In this article, we take into account the fractional space Kundu–Mukherjee–Naskar model with time-dependent coefficients (FSKMNE-TDCs). By incorporating time-dependent coefficients (TDCs) into the equation, researchers can better model systems that exhibit nonconstant or nonlinear behavior over time. This has important implications for understanding complex phenomena such as turbulence in fluid flow, quantum tunneling in particle physics, and time-varying electromagnetic fields. We apply the mapping method to obtain hyperbolic, elliptic, trigonometric and rational fractional solutions. These solutions are vital for understanding some fundamentally complicated phenomena. The obtained solutions will be very helpful for applications such as optical fiber wave propagation in a magnetized plasma, oceanic rogue waves, and ion-acoustic waves. Finally, we show how the M-truncated derivative order and TDCs affect the exact solution of the FSKMNE-TDCs.

Keywords: exact solutions, random coefficient, M-truncated derivative operator, mapping method

1 Introduction

Fractional differential equations (FDEs) lie in their ability to capture nonlocal and memory effects through derivatives of noninteger order. These equations have a wide range of applications and are employed in physics, biology, medicine, engineering, and finance [1–7]. In physics, these equations can describe complex systems, such as fluid dynamics, electromagnetic theory, and quantum mechanics. Fractional calculus provides a powerful mathematical tool for modeling and analyzing fractional physical systems. Moreover, FDEs have proven to be useful in engineering fields where they are utilized in the design and analysis of control systems, signal processing, and image-processing applications. Fractional derivatives can describe the behavior of viscoelastic materials, allowing engineers to design more effective materials and structures.

On the other side, partial differential equations (PDEs) with variable coefficients play a crucial role in various fields of science and engineering. These equations involve functions with multiple independent variables and their partial derivatives. The coefficients in these equations are not constant but vary with the independent variables. This variation allows for a more accurate representation of real-world phenomena and provides a deeper understanding of complex systems.

Moreover, solving PDEs with variable coefficients remains a challenging task. Recently, there are various helpful and practical techniques for solving these equations, including the (G'/G)-expansion method [8], the sub-equation method [9], the Hirota's bilinear approach [10], the (G'/G^2)-expansion and Jacobian elliptic functions methods [11], solitary wave ansatz [12]. Moreover, there are many methods for solving PDEs with constant coefficients, for example, the extended (G'/G)-expansion method [13,14], the generalized Kudryashov approach [15], the $(G'/G, 1/G)$-expansion method [16], the $\exp(-\varphi(\eta))$-expansion method [17], the generalized Riccati equation mapping method [18], the Lie symmetry method [19], the multivariate generalized exponential rational integral function [20], the modified generalized Riccati equation mapping approach [21], the generalized exponential rational function method [22], the generalized Riccati equation [23], and the He's semi-inverse method [24,25].

To achieve a better degree of qualitative agreement, we consider here the fractional-space Kundu–Mukherjee–Naskar equation (FSKMNE) with time-dependent coefficients (TDCs) as follows:

* **Corresponding author: Farah M. Al-Askar,** Department of Mathematical Science, Collage of Science, Princess Nourah bint Abdulrahman University, P.O. Box 84428, Riyadh 11671, Saudi Arabia, e-mail: famalaskar@pnu.edu.sa

$$i\mathcal{W}_t + a(t)\mathcal{T}^{\alpha,\delta}_{xy}\mathcal{W} + ib(t)[\mathcal{W}\mathcal{T}^{\alpha,\delta}_{x}\mathcal{W}^* - \mathcal{W}^*\mathcal{T}^{\alpha,\delta}_{x}\mathcal{W}]\mathcal{W} = 0, \tag{1}$$

where $\mathcal{W}$ is the optical soliton profile, $\mathcal{T}^{\alpha,\delta}$ is M-truncated derivative (MTD) operator, and $a(t)$ and $b(t)$ are arbitrary functions of the variable t.

In 2013, Kundu and Mukherjee [26] suggested Eq. (1) with $\delta = 0$ and $\alpha = 1$. It is derived from the basic hydrodynamic equations as a two-dimensional nonlinear Schrödinger equation. This Eq. (1) can be used to illustrate optical fiber wave propagation, oceanic rogue waves and ion-acoustic waves in a magnetized plasma [27–29]. Numerous studies have been carried out on Eq. (1) to examine soliton propagation into an optical fiber. As a consequence, several mathematical approaches are utilized to obtain exact solutions, such as (G'/G)-expansion method [30], Lie symmetry [31], Jacobi elliptic functions [32], extended trial function [33], modified simple equation [34], and trial equation [35].

The motivation of this article is to establish the exact solutions of the FSKMNE-TDCs (1). We employ the mapping approach to acquired a variety of solutions for instance trigonometric, hyperbolic, rational, and elliptic functions. The acquired solutions are very helpful for applications such as optical fiber wave propagation in a magnetized plasma, oceanic rogue waves, and ion-acoustic waves. Furthermore, we use Matlab program to produce 2D and 3D figures for some of the analytical solutions established in this work to examine the impact of the MTD and TDC on the acquired solutions of the FSKMNE-TDCs (1).

This article is organized as follows: In Section 2, we define the MTD and describe some of its characteristics. To obtain the wave equation of the SFSKMN-TDCs (1), we use a suitable wave transformation in Section 3. In Section 4, we construct the exact solutions of the SFSKMN-TDCs using the mapping method (1). In Section 5, we address the impact of the MTD on the attained solutions. Finally, the conclusion of the article is presented.

2 M-truncated fractional derivative

Fractional calculus operators are an effective tool for modeling and evaluating complicated processes that cannot be effectively explained using regular integer-order calculus. Several forms of fractional derivative operators have been suggested in the literature, including the Katugampola derivative, the Jumarie derivative, the Hadamard derivative, the Caputo derivative, the Riemann–Liouville derivative, and the Grünwald–Letnikov derivative [36–39]. In recent years, Sousa and de Oliveira [40] introduced a novel derivative known as the MTD that arises naturally from the classical derivative. The MTD exhibits several classical calculus features, such as the function composition rule, chain rule, product rule, linearity, and quotient rule. The MTD for $u : [0, \infty) \to \mathbb{R}$ of order $0 < \alpha \le 1$ is given as follows:

$$\mathcal{T}^{\alpha,\delta}_{x}\mathcal{U}(x) = \lim_{h\to 0}\frac{\mathcal{U}(x\mathcal{E}_{k,\delta}(hx^{-\alpha})) - \mathcal{U}(x)}{h},$$

where

$$\mathcal{E}_{k,\delta}(z) = \sum_{j=0}^{k}\frac{z^j}{\Gamma(\delta j + 1)}, \quad \text{for } z \in \mathbb{C} \quad \text{and} \quad \delta > 0.$$

The MTD has the next features for any real constants a and b [40]:

(1) $\mathcal{T}^{\alpha,\delta}_{x}(a\mathcal{U} + b\mathcal{V}) = a\mathcal{T}^{\alpha,\delta}_{x}\mathcal{U} + b\mathcal{T}^{\alpha,\delta}_{x}\mathcal{V}$,

(2) $\mathcal{T}^{\alpha,\delta}_{x}(\mathcal{U} \circ \mathcal{V})(x) = \mathcal{U}'(\mathcal{V}(x))\mathcal{T}^{\alpha,\delta}_{x}\mathcal{U}(x)$,

(3) $\mathcal{T}^{\alpha,\delta}_{x}(\mathcal{U}\mathcal{V}) = \mathcal{U}\mathcal{T}^{\alpha,\delta}_{x}\mathcal{V} + \mathcal{V}\mathcal{T}^{\alpha,\delta}_{x}\mathcal{U}$,

(4) $\mathcal{T}^{\alpha,\delta}_{x}\mathcal{U}(x) = \frac{x^{1-\alpha}}{\Gamma(\beta+1)}\frac{d\mathcal{U}}{dx}$,

(5) $\mathcal{T}^{\alpha,\delta}_{x}(x^{\nu}) = \frac{\nu}{\Gamma(\beta+1)}x^{\nu-\alpha}$.

3 Wave equation for FSKMN-TDCs

To acquire the wave equation for the FSKMN-TDCs (1), the next wave transformation is applied:

$$\mathcal{W}(x, y, t) = \mathcal{G}(\mu_\alpha)e^{i\psi_\alpha}, \tag{2}$$

$$\mu_\alpha = \frac{\Gamma(1+\delta)}{\alpha}[\mu_1 x^\alpha + \mu_2 y^\alpha] + \int_0^t f(\tau)d\tau,$$

and

$$\psi_\alpha = \frac{\Gamma(1+\delta)}{\alpha}[\rho_1 x^\alpha + \rho_2 y^\alpha] + \int_0^t g(\tau)d\tau,$$

where $\mathcal{G}$ is a real valued function. Plugging Eq. (2) into Eq. (1) and using

$$\frac{\partial\mathcal{W}}{\partial t} = [f(t)\mathcal{G}' + ig(t)\mathcal{G}]e^{i\psi_\alpha},$$
$$\mathcal{T}^{\alpha}_{x}\mathcal{W} = (\mu_1\mathcal{G}' + i\rho_1\mathcal{G})e^{i\psi_\alpha}, \mathcal{T}^{\alpha}_{x}\mathcal{W}^* = (\mu_1\mathcal{G}' - i\rho_1\mathcal{G})e^{-i\psi_\alpha}$$
$$\mathcal{T}^{\alpha}_{xy}\mathcal{W} = [\mu_1\mu_2\mathcal{G}'' + i(\rho_1\mu_2 + \rho_2\mu_1)\mathcal{G}' - \rho_1\rho_2\mathcal{G}]e^{i\psi_\alpha},$$

we obtain for imaginary part

$$[f(t) + a(t)(\rho_1\mu_2 + \rho_2\mu_1)]\mathcal{G}' = 0, \tag{3}$$

and for real part

$$\mu_1\mu_2 a(t)\mathcal{G}'' - (g(t) + \rho_1\rho_2 a(t))\mathcal{G} + 2\rho_1 b(t)\mathcal{G}^3 = 0. \tag{4}$$

From (3), we obtain

$$f(t) = -(\rho_1\mu_2 + \rho_2\mu_1)a(t). \tag{5}$$

4 The analytical solutions of the SFKMNE

Here, the mapping method, which was reported by Peng [41], is used. Let the solutions of Eq. (4) have the form

$$\mathcal{G}(\mu_a) = \sum_{i=0}^{K} \ell_i(t)\mathcal{U}^i(\mu_a), \tag{6}$$

where $\ell_i(t)$ are unknown functions in t for $i = 0, 1, \ldots, K$, and $\mathcal{U}$ is the solution of

$$\mathcal{U}' = \sqrt{\hbar_1\mathcal{U}^4 + \hbar_2\mathcal{U}^2 + \hbar_3}, \tag{7}$$

where $\hbar_1$, $\hbar_2$, and $\hbar_3$ are real constants.

By balancing $\mathcal{G}''$ with $\mathcal{G}^3$ in Eq. (4), we can determine K as follows:

$$K + 2 = 3K \Rightarrow K = 1.$$

With $K = 1$, Eq. (6) becomes

$$\mathcal{G}(\mu_a) = \ell_0(t) + \ell_1(t)\mathcal{U}(\mu_a). \tag{8}$$

Differentiating Eq. (8) twice and using (7), we obtain

$$\mathcal{G}'' = \ell_1(\hbar_2\mathcal{U} + 2\hbar_1\mathcal{U}^3). \tag{9}$$

By substituting Eqs. (8) and (9) into Eq. (4), we have

$$\begin{aligned}&[2\mu_1\mu_2\ell_1\hbar_1 a(t) + 2\rho_1\ell_1^3 b(t)]\mathcal{U}^3 + 6\rho_1 b(t)\ell_0\ell_1^2\mathcal{U}^2\\ &+ [\mu_1\mu_2\ell_1\hbar_2 a(t) + 6\rho_1\ell_0^2\ell_1 b(t) - \ell_1(g(t) + \rho_1\rho_2 a(t))]\mathcal{U}\\ &+ [2\rho_1\ell_0^3 b(t) - \ell_0(g(t) + \rho_1\rho_2 a(t))] = 0.\end{aligned}$$

For $i = 3, 2, 1, 0$, we put all coefficient of $\mathcal{U}^i$ equal zero to attain

$$2\mu_1\mu_2\ell_1\hbar_1 a(t) + 2\rho_1\ell_1^3 b(t) = 0,$$

$$6\rho_1 b(t)\ell_0\ell_1^2 = 0,$$

$$\mu_1\mu_2\ell_1\hbar_2 a(t) + 6\rho_1\ell_0^2\ell_1 b(t) - \ell_1(g(t) + \rho_1\rho_2 a(t)) = 0,$$

and

$$2\rho_1\ell_0^3 b(t) - \ell_0(g(t) + \rho_1\rho_2 a(t)) = 0.$$

When we solve these equations, we obtain three different sets:

$$\begin{aligned}&\ell_0(t) = 0, \quad \ell_1(t) = \pm\sqrt{\frac{-\mu_1\mu_2\hbar_1 a(t)}{\rho_1 b(t)}},\\ &g(t) = (\mu_1\mu_2\hbar_2 - \rho_1\rho_2)a(t),\end{aligned} \tag{10}$$

and

$$f(t) = -(\rho_1\mu_2 + \rho_2\mu_1)a(t). \tag{11}$$

By utilizing Eqs. (2), (8), and (10), the solution of FSKMNE-TDCs (1) is expressed as follows:

$$\mathcal{W}(x, y, t) = \pm\sqrt{\frac{-\mu_1\mu_2\hbar_1 a(t)}{\rho_1 b(t)}}\,\mathcal{U}(\mu_a)e^{i\psi_a}, \tag{12}$$

where

$$\mu_a = \frac{\Gamma(1+\delta)}{\alpha}[\mu_1 x^\alpha + \mu_2 y^\alpha] - (\rho_1\mu_2 + \rho_2\mu_1)\int_0^t a(\tau)\mathrm{d}\tau$$

and

$$\psi_a = \frac{\Gamma(1+\delta)}{\alpha}[\rho_1 x^\alpha + \rho_2 y^\alpha] + (\mu_1\mu_2\hbar_2 - \rho_1\rho_2)\int_0^t a(\tau)\mathrm{d}\tau.$$

There are many sets depending on $\hbar_1$, $\hbar_2$, and $\hbar_3$:

Set 1: If $\hbar_1 = m^2$, $\hbar_2 = -(1 + m^2)$ and $\hbar_3 = 1$, then $\mathcal{U}(\xi) = sn(\mu_a)$. Therefore, the solution of FSKMN-TDCs (1), by using Eq. (12), is given as follows:

$$\mathcal{W}(x, y, t) = \pm m\sqrt{\frac{-\mu_1\mu_2 a(t)}{\rho_1 b(t)}}\,sn(\mu_a)e^{i\psi_a} \quad \text{if } \frac{\mu_1\mu_2 a(t)}{\rho_1 b(t)} < 0 \quad \text{for all } t > 0. \tag{13}$$

At $m \to 1$, Eq. (13) becomes

$$\mathcal{W}(x, y, t) = \pm\sqrt{\frac{-\mu_1\mu_2 a(t)}{\rho_1 b(t)}}\,\tanh(\mu_a)e^{i\psi_a} \quad \text{if } \frac{\mu_1\mu_2 a(t)}{\rho_1 b(t)} < 0 \quad \text{for all } t > 0. \tag{14}$$

Set 2: If $\hbar_1 = 1$, $\hbar_2 = 2m^2 - 1$ and $\hbar_3 = -m^2(1 - m^2)$, then $\mathcal{U}(\mu_a) = ds(\mu_a)$. Consequently, the solution of FSKMN-TDCs (1), by using Eq. (12), is given as follows:

$$\mathcal{W}(x, y, t) = \pm\sqrt{\frac{-\mu_1\mu_2 a(t)}{\rho_1 b(t)}}\,\mathrm{ds}(\mu_a)e^{i\psi_a} \quad \text{if } \frac{\mu_1\mu_2 a(t)}{\rho_1 b(t)} < 0 \quad \text{for all } t > 0. \tag{15}$$

When $m \to 1$, Eq. (15) is typically

$$\mathcal{W}(x, y, t) = \pm\sqrt{\frac{-\mu_1\mu_2 a(t)}{\rho_1 b(t)}}\,\mathrm{csch}(\mu_a)e^{i\psi_a} \quad \text{if } \frac{\mu_1\mu_2 a(t)}{\rho_1 b(t)} < 0 \quad \text{for all } t > 0. \tag{16}$$

At $m \to 0$, Eq. (15) tends to

$$\mathcal{W}(x, y, t) = \pm\sqrt{\frac{-\mu_1\mu_2 a(t)}{\rho_1 b(t)}}\,\csc(\mu_a)e^{i\psi_a} \quad \text{if } \frac{\mu_1\mu_2 a(t)}{\rho_1 b(t)} < 0 \quad \text{for all } t > 0. \tag{17}$$

Set 3: If $\hbar_1 = 1, \hbar_2 = 2 - m^2$, and $\hbar_3 = (1 - m^2)$, then $\mathcal{U}(\mu_a) = cs(\mu_a)$. Therefore, the solution of FSKMN-TDCs (1) is expressed as follows:

$$\mathcal{W}(x, y, t) = \pm\sqrt{\frac{-\mu_1\mu_2 a(t)}{\rho_1 b(t)}}\, cs(\mu_a)e^{i\psi_a}$$
$$\text{if } \frac{\mu_1\mu_2 a(t)}{\rho_1 b(t)} < 0 \quad \text{for all } t > 0. \tag{18}$$

At $m \to 1$, Eq. (18) is typically

$$\mathcal{W}(x, y, t) = \pm\sqrt{\frac{-\mu_1\mu_2 a(t)}{\rho_1 b(t)}}\, \text{csch}(\mu_a)e^{i\psi_a}$$
$$\text{if } \frac{\mu_1\mu_2 a(t)}{\rho_1 b(t)} < 0 \quad \text{for all } t > 0. \tag{19}$$

If $m \to 0$, then Eq. (18) becomes

$$\mathcal{W}(x, y, t) = \pm\sqrt{\frac{-\mu_1\mu_2 a(t)}{\rho_1 b(t)}}\, \cot(\mu_a)e^{i\psi_a}$$
$$\text{if } \frac{\mu_1\mu_2 a(t)}{\rho_1 b(t)} < 0 \quad \text{for all } t > 0. \tag{20}$$

Set 4: If $\hbar_1 = \frac{m^2}{4}, \hbar_2 = \frac{(m^2-2)}{2}$ and $\hbar_3 = \frac{1}{4}$, then $\mathcal{U}(\mu_a) = \frac{sn(\mu_a)}{1+dn(\mu_a)}$. Consequently, the solution of FSKMN-TDCs (1) is given as follows:

$$\mathcal{W}(x, y, t) = \pm\frac{m}{2}\sqrt{\frac{-\mu_1\mu_2 a(t)}{\rho_1 b(t)}}\, \frac{sn(\mu_a)}{1 + dn(\mu_a)}e^{i\psi_a}$$
$$\text{if } \frac{\mu_1\mu_2 a(t)}{\rho_1 b(t)} < 0 \quad \text{for all } t > 0. \tag{21}$$

At $m \to 1$, Eq. (21) tends to

$$\mathcal{W}(x, y, t) = \pm\frac{1}{2}\sqrt{\frac{-\mu_1\mu_2 a(t)}{\rho_1 b(t)}}\, \frac{\tanh(\mu_a)}{1 + \text{sech}(\mu_a)}e^{i\psi_a}$$
$$\text{if } \frac{\mu_1\mu_2 a(t)}{\rho_1 b(t)} < 0 \quad \text{for all } t > 0. \tag{22}$$

Set 5: If $\hbar_1 = \frac{(1-m^2)^2}{4}, \hbar_2 = \frac{(1-m^2)^2}{2}$, and $\hbar_3 = \frac{1}{4}$, then $\mathcal{U}(\mu_a) = \frac{sn(\mu_a)}{dn(\mu_a)+cn(\mu_a)}$. Therefore, the solution of FSKMN-TDCs (1) is given as follows:

$$\mathcal{W}(x, y, t) = \pm\frac{(1 - m^2)}{2}\sqrt{\frac{-\mu_1\mu_2 a(t)}{\rho_1 b(t)}}\left[\frac{sn(\mu_a)}{dn(\mu_a) + cn(\mu_a)}\right]e^{i\psi_a} \tag{23}$$
$$\text{if } \frac{\mu_1\mu_2 a(t)}{\rho_1 b(t)} < 0 \quad \text{for all } t > 0.$$

If $m \to 0$, then Eq. (23) is typically

$$\mathcal{W}(x, y, t) = \pm\frac{1}{2}\sqrt{\frac{-\mu_1\mu_2 a(t)}{\rho_1 b(t)}}\left[\frac{\sin(\mu_a)}{1 + \cos(\mu_a)}\right]e^{i\psi_a}$$
$$\text{if } \frac{\mu_1\mu_2 a(t)}{\rho_1 b(t)} < 0 \quad \text{for all } t > 0. \tag{24}$$

Set 6: If $\hbar_1 = \frac{1-m^2}{4}, \hbar_2 = \frac{(1-m^2)}{2}$, and $\hbar_3 = \frac{1-m^2}{4}$, then $\mathcal{U}(\mu_a) = \frac{cn(\mu_a)}{1+sn(\mu_a)}$. Consequently, the solution of FSKMN-TDCs (1) is given as follows:

$$\mathcal{W}(x, y, t) = \pm\frac{1}{2}\sqrt{\frac{-(1 - m^2)\mu_1\mu_2 a(t)}{\rho_1 b(t)}}\left[\frac{cn(\mu_a)}{1 + sn(\mu_a)}\right]e^{i\psi_a}$$
$$\text{if } \frac{\mu_1\mu_2 a(t)}{\rho_1 b(t)} < 0 \quad \text{for all } t > 0. \tag{25}$$

At $m \to 0$, Eq. (25) turns to

$$\mathcal{W}(x, y, t) = \pm\frac{1}{2}\sqrt{\frac{-\mu_1\mu_2 a(t)}{\rho_1 b(t)}}\left[\frac{\cos(\mu_a)}{1 + \sin(\mu_a)}\right]e^{i\psi_a}$$
$$\text{if } \frac{\mu_1\mu_2 a(t)}{\rho_1 b(t)} < 0 \quad \text{for all } t > 0. \tag{26}$$

Set 7: If $\hbar_1 = 1, \hbar_2 = 0$, and $\hbar_3 = 0$, then $\mathcal{U}(\mu_a) = \frac{c}{\mu_a}$. Therefore, the solution of FSKMN-TDCs (1) is

$$\mathcal{W}(x, y, t) = \pm\sqrt{\frac{-\mu_1\mu_2 a(t)}{\rho_1 b(t)}}\left[\frac{c}{\mu_a}\right]e^{i\psi_a}$$
$$\text{if } \frac{\mu_1\mu_2 a(t)}{\rho_1 b(t)} < 0 \quad \text{for all } t > 0. \tag{27}$$

Set 8: If $\hbar_1 = -m^2, \hbar_2 = 2m^2 - 1$, and $\hbar_3 = 1 - m^2$, then $\mathcal{U}(\mu_a) = cn(\mu_a)$. Consequently, the solution of FSKMN-TDCs (1) is given as follows:

$$\mathcal{W}(x, y, t) = \pm m\sqrt{\frac{\mu_1\mu_2 a(t)}{\rho_1 b(t)}}\, [cn(\mu_a)]e^{i\psi_a}$$
$$\text{if } \frac{\mu_1\mu_2 a(t)}{\rho_1 b(t)} > 0 \quad \text{for all } t > 0. \tag{28}$$

When $m \to 1$, Eq. (28) is typically

$$\mathcal{W}(x, y, t) = \pm\sqrt{\frac{\mu_1\mu_2 a(t)}{\rho_1 b(t)}}\, [\text{sech}(\mu_a)]e^{i\psi_a}$$
$$\text{if } \frac{\mu_1\mu_2 a(t)}{\rho_1 b(t)} > 0 \quad \text{for all } t > 0. \tag{29}$$

Set 9: If $\hbar_1 = \frac{-1}{4}, \hbar_2 = \frac{m^2+1}{2}$, and $\hbar_3 = \frac{-(1-m^2)^2}{2}$, then $\mathcal{U}(\mu_a) = mcn(\mu_a) + dn(\mu_a)$. Therefore, the solution of FSKMN-TDCs (1) is given as follows:

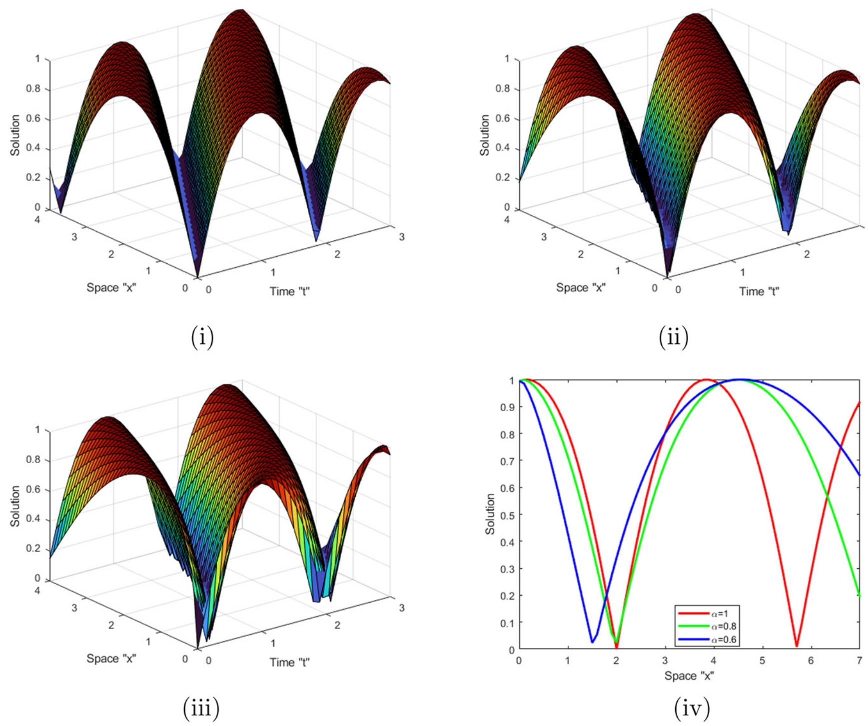

Figure 1: (i)–(iii) 3D profile of the periodic solution $|\mathcal{W}(x,y,t)|$ described in Eq. (13) with $\alpha = 1, 0.8, 0.6$ (iv) depict 2D profile of Eq. (13) with various values of α. (i) $\alpha = 1$, (ii) $\alpha = 0.8$, (iii) $\alpha = 0.6$, and (iv) $\alpha = 1, 0.8, 0.6$.

$$\mathcal{W}(x,y,t) = \pm\frac{1}{2}\sqrt{\frac{\mu_1\mu_2 a(t)}{\rho_1 b(t)}}[mcn(\mu_\alpha) + dn(\mu_\alpha)]e^{i\psi_\alpha}$$
$$\text{if } \frac{\mu_1\mu_2 a(t)}{\rho_1 b(t)} > 0 \quad \text{for all } t > 0. \tag{30}$$

When $m \to 1$, Eq. (30) tends to Eq. (29).

Set 10: If $\hbar_1 = \frac{m^2-1}{4}$, $\hbar_2 = \frac{m^2+1}{2}$, and $\hbar_3 = \frac{m^2-1}{4}$, then $\mathcal{U}(\mu_\alpha) = \frac{\mathrm{dn}(\mu_\alpha)}{1+sn(\mu_\alpha)}$. Hence, the solution of FSKMN-TDCs (1) is given as follows:

$$\mathcal{W}(x,y,t) = \pm\frac{1}{2}\sqrt{\frac{(1-m^2)\mu_1\mu_2 a(t)}{\rho_1 b(t)}}\left[\frac{\mathrm{dn}(\mu_\alpha)}{1+sn(\mu_\alpha)}\right]e^{i\psi_\alpha}$$
$$\text{if } \frac{\mu_1\mu_2 a(t)}{\rho_1 b(t)} > 0 \quad \text{for all } t > 0. \tag{31}$$

When $m \to 0$, Eq. (31) is typically

$$\mathcal{W}(x,y,t) = \pm\frac{1}{2}\sqrt{\frac{\mu_1\mu_2 a(t)}{\rho_1 b(t)}}\left[\frac{1}{1+\sin(\mu_\alpha)}\right]e^{i\psi_\alpha}$$
$$\text{if } \frac{\mu_1\mu_2 a(t)}{\rho_1 b(t)} > 0 \quad \text{for all } t > 0. \tag{32}$$

Set 11: If $\hbar_1 = -1$, $\hbar_2 = 2 - m^2$, and $\hbar_3 = m^2 - 1$, then $\mathcal{U}(\mu_\alpha) = dn(\mu_\alpha)$. Therefore, the solution of FSKMN-TDCs (1) is given as follows:

$$\mathcal{W}(x,y,t) = \pm\sqrt{\frac{\mu_1\mu_2 a(t)}{\rho_1 b(t)}}[dn(\mu_\alpha)]e^{i\psi_\alpha}$$
$$\text{if } \frac{\mu_1\mu_2 a(t)}{\rho_1 b(t)} > 0 \quad \text{for all } t > 0. \tag{33}$$

If $m \to 1$, then Eq. (33) turns to Eq. (29).

Remark 1. Putting $\alpha = 1$, $a(t) = a$, $b(t) = b$, $\mu_1 = B_1$, $\mu_2 = B_2$, $\rho_1 = k_1$, $\rho_2 = k_2$, and $f(t) = -\rho$ in Eqs. (16), (20), and (29), we have the same results that stated in [34].

5 Impact of MTD and physical meaning

Impacts of MTD: Now, we study the impact of MTD on the acquired solutions of the FSKMN-TDCs (1). A series of two-dimensional and three-dimensional graphs are generated by assigning suitable values to the unknown variables. Figures 1 and 2 represent the behavior solutions of (13), and (14), respectively. Figure 1 displays the periodic solutions $|\mathcal{W}(x,y,t)|$ described in Eq. (13) for $\mu_1 = \rho_2 = -1$, $\rho_1 = \mu_2 = 1$, $a(t) = t$, $b(t) = t$, $\delta = 0.9$, $x \in [0,4]$, $t \in [0,3]$ and for $\alpha = 1, 0.8, 0.6$. While Figure 2 displays the bright solutions $|\mathcal{W}(x,y,t)|$ described in Eq. (14) for $\mu_1=\rho_2=-1$, $\rho_1=\mu_2=1$, $a(t)=t$, $b(t)=t$, $x\in[0,4]$, $y=0$, $t\in[0,3]$ and for $\alpha=1, 0.8, 0.6$. From these figures, we deduce that when the derivative order α of MTD decreases, the surface moves into the left side.

Impacts of TDCs: Now, we study the impact of the TDCs on the acquired solutions of the FSKMN-TDCs (1). Figures 3 and 4 display the solutions $|\mathcal{W}(x,y,t)|$ described in Eqs. (13) and (14) for $\mu_1=\rho_2=-1, \rho_1=\mu_2=1, \delta=0$, $x\in[0,4]$, $y=0$, $t\in[0,3]$ and for $\alpha=1$. In Figures 3(i) and 4(i), we assume $a(t)=b(t)=t$, and this choice makes the surface twist from the left. In Figures 3(ii) and 4(ii), we assume $a(t)=1, b(t)=\sinh(t)$, and this option makes the surface a little flat from the right. In Figures 3(iii) and 4(iii), we assume $a(t)=\cos(t), b(t)=1$, and this choise effects on the surface sides. While in Figures 3(v) and 4(v), we assume $a(t)=b(t)=W_t(t)$, where $W_t(t)$ is the derivative of Wiener process $W(t)$, and this option causes the surface to oscillate.

Physical meaning: The Kundu–Mukherjee–Naskar equation with TDCs offers a powerful tool for optimizing processes or designing new technologies. By modeling the time-dependent behavior of a system accurately, researchers can identify critical points in the system where improvements can be made or where potential issues may arise. This can lead to more efficient processes, increased reliability, and better performance in a wide range of applications, from aerospace engineering to biomedical research. Therefore, the exact solutions of the FSKMNE-TDCs (1) were acquired here. We applied the mapping method, which provided many types of solutions including periodic solutions, kink solutions, bright solutions, dark optical solution, singular solution, *etc*.

6 Conclusions

In this article, we considered FSKMNE-TDCs (1). One of the key advantages of the Kundu–Mukherjee–Naskar equation with time-dependent coefficients is its ability to capture the dynamic behavior of physical systems. By incorporating TDCs into the equation, researchers can better model systems that exhibit nonconstant or nonlinear behavior over time. This has important implications for understanding complex phenomena such as turbulence in fluid flow, quantum tunneling in particle physics, and time-varying electromagnetic fields. We applied the mapping method to obtain hyperbolic, elliptic, trigonometric, and rational fractional solutions. These solutions are important for understanding some fundamentally complicated phenomena. The acquired solutions are very helpful for applications such as optical fiber wave propagation in a magnetized

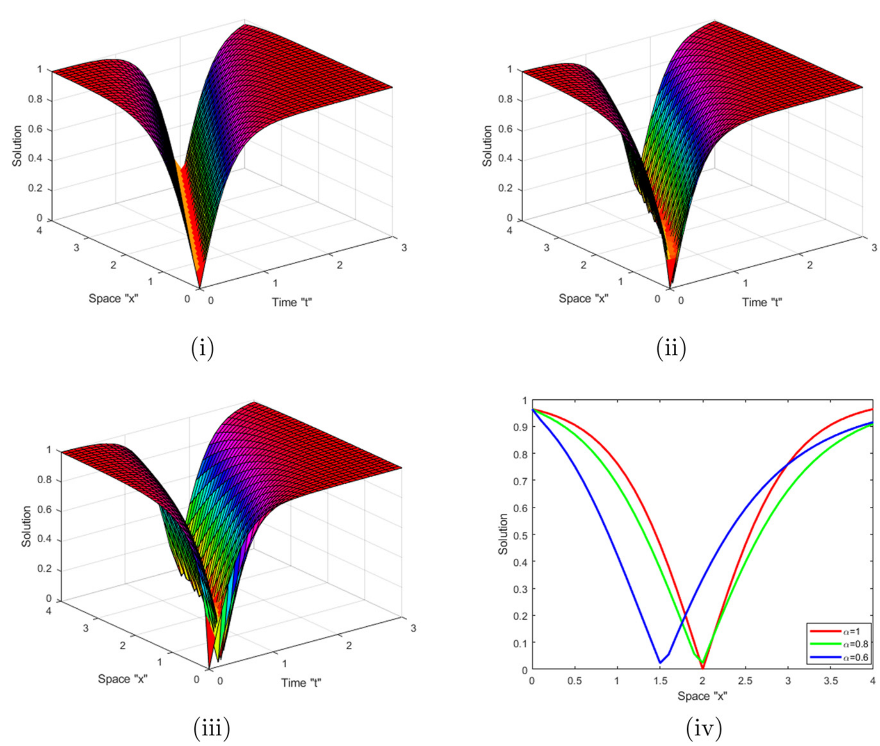

(i) (ii) (iii) (iv)

Figure 2: (i)–(iii) 3D-profile of the bright solution $|\mathcal{W}(x,y,t)|$ described in Eq. (14) with $\alpha=1, 0.8, 0.6$ (iv) depict 2D-profile of Eq. (14) with various α. (i) $\alpha=1$, (ii) $\alpha=0.8$, (iii) $\alpha=0.6$, and (iv) $\alpha=1, 0.8, 0.6$.

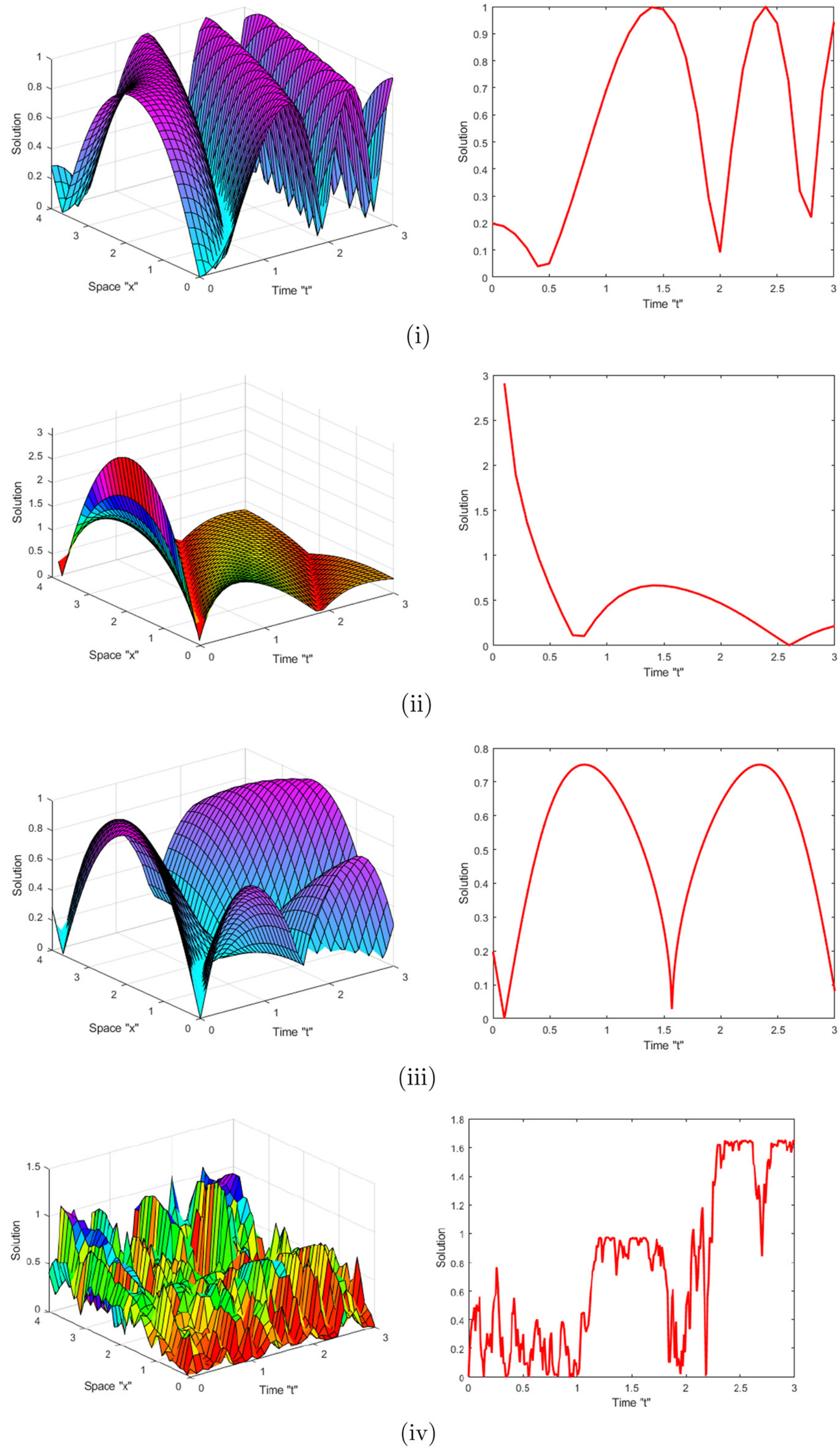

Figure 3: 3D and 2D profile for the solution $|\mathcal{W}(x, y, t)|$ stated in Eq. (13) with different TDCs. (i) $a(t) = t$, $b(t) = t$, (ii) $a(t) = 1$, $b(t) = \sinh(t)$, (iii) $a(t) = \cos(t)$, $b(t) = 1$, and (v) $a(t) = W_t$, $b(t) = W_t$.

plasma, oceanic rogue waves, and ion-acoustic waves. Finally, we show how the MTD order affects the exact solution of the FSKMNE-TDCs (1). We deduced that when the derivative order α of MTD decreases, the surface moves into the left side. In the future work, we can study (1) with the stochastic term.

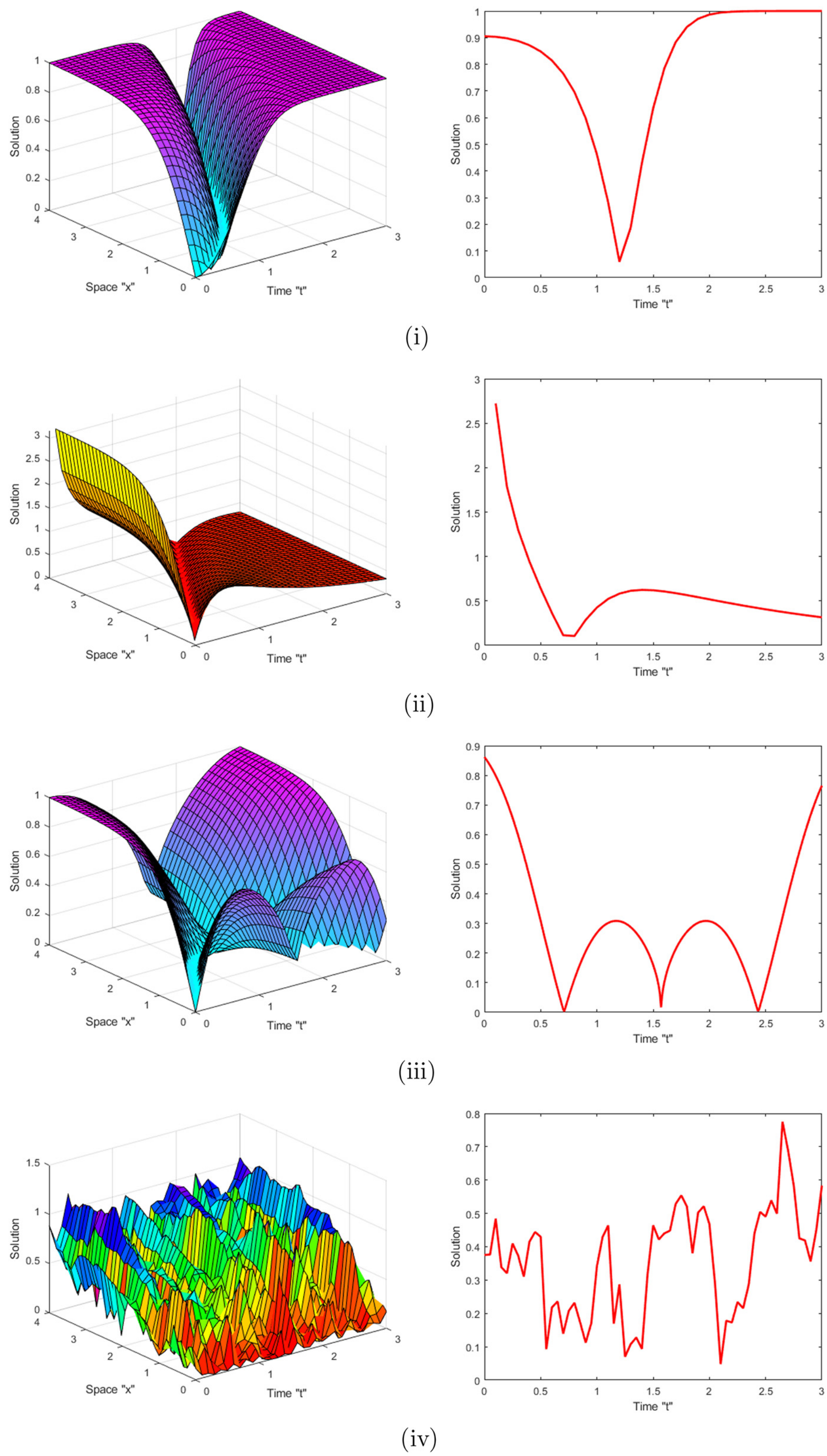

Figure 4: 3D and 2D profile for the solution $|\mathcal{W}(x,y,t)|$ stated in Eq. (14) with different TDCs. (i) $a(t) = t$, $b(t) = t$, (ii) $a(t) = 1$, $b(t) = \sinh(t)$, (iii) $a(t) = \cos(t)$, $b(t) = 1$, and (v) $a(t) = W_t$, $b(t) = W_t$.

Acknowledgments: Princess Nourah bint Abdulrahman University Researcher Supporting Project number (PNURSP2024R 273), Princess Nourah bint Abdulrahman University, Riyadh, Saudi Arabia.

Funding information: Princess Nourah bint Abdulrahman University Researcher Supporting Project number (PNURSP2024R 273), Princess Nourah bint Abdulrahman University, Riyadh, Saudi Arabia.

Author contributions: All authors have accepted responsibility for the entire content of this manuscript and approved its submission.

Conflict of interest: The author states no conflict of interest.

Data availability statement: All data generated or analysed during this study are included in this published article.

References

[1] Oldham KB, Spanier J. The fractional calculus: Theory and applications of differentiation and ntegration to Arbitrary Order, vol. 11 of Mathematics in Science and Engineering, New York, NY, USA: Academic Press; 1974.
[2] Miller KS, Ross B. An introduction to the fractional calculus and fractional differential equations, New York, NY, USA: A Wiley-Interscience Publication, John Wiley & Sons; 1993.
[3] Mohammed WW, Cesarano C, Iqbal N, Sidaoui R, Ali EE. The exact solutions for the fractional Riemann wave equation in quantum mechanics and optics. Phys Scr. 2024;99:085245.
[4] Hilfer R. Applications of fractional calculus in physics, Singapore: World Scientific Publishing; 2000.
[5] Mohammed WW, Cesarano C, Elsayed EM, Al-Askar FM. The analytical fractional solutions for coupled Fokas system in fiber optics using different methods. Fractal Fract. 2023;7:556.
[6] Mohammadi H, Kumar S, Rezapour S, Etemad S. A theoretical study of the Caputo-Fabrizio fractional modeling for hearing loss due to Mumps virus with optimal control. Chaos Soliton Fract. 2021;144:110668.
[7] Alshammari M, Hamza AE, Cesarano C, Aly ES, Mohammed WW. The analytical solutions to the fractional Kraenkel-Manna-Merle system in ferromagnetic materials. Fractal Fract. 2023;7(7):523.
[8] Al-Askar FM. New solutions to the fractional perturbed Chen Lee Liu model with time-dependent coefficients: Applications to complex phenomena in optical fibers. Contemp Math. 2024;5:4697.
[9] Injrou S. Exact solutions for the Conformable space-time fractional Zeldovich equation with time-dependent coefficients. Int J Differ Equ. 2022;2020:9312830.
[10] Ismael HF, Nabi HR, Sulaiman TA, Shah NA, Ali MR. Multiple soliton and M-lump waves to a generalized B-type Kadomtsev-Petviashvili equation. Results Phys. 2023;48:106402.
[11] Qi J, Zhu Q. Further results about the non-traveling wave exact solutions of nonlinear Burgers equation with variable coefficients. Results Phys. 2023;46:106285.
[12] Mohammed WW, Iqbal N, Bourazza S, Elsayed EM. The optical structures for the fractional chiral nonlinear Schrödinger equation with time-dependent coefficients. Opt Quant Electron. 2024;56:1476.
[13] Roshid HO, Rahman N, Ali Akbar MA. Traveling waves solutions of nonlinear Klein Gordon equation by extended (G'/G)-expasion method. Ann Pure Appl Math. 2013;3:10–6.
[14] Roshid HO, Akbar MA, Alam MN, Hoque FMd, Rahman N. New extended $(G^{'}/G)$-expansion method to solve nonlinear evolution equation: the (3 + 1)-dimensional potential-YTSF equation. SpringerPlus. 2014;3:122.
[15] Barman HK, Roy R, Mahmud F, Akbar MA, Osman MS. Harmonizing wave solutions to the Fokas-Lenells model through the generalized Kudryashov method. Optik. 2021;229:166294.
[16] Miah MM, Shahadat HM, Ali HM, Akbar MA, Seadawy AR. New applications of the two variable $(G'/G, 1/G)$-expansion method for closed form traveling wave solutions of integro-differential equations. J Ocean Eng Sci. 2019;4:132–43.
[17] Alam MN, Hafez MG, Akbar MA, Roshid HO. Exact traveling wave solutions to the (3+1)-dimensional mKdV-ZK and the (2+1)-dimensional Burgers equations via $\exp(\varphi(\eta))$-expansion method. Alex Eng J. 2015;54:635–44.
[18] Kumar S, Mann N. A variety of newly formed soliton solutions and patterns of dynamic waveforms for the generalized complex coupled Schrödinger-Boussinesq equations. Opt Quant Electron. 2023;55:723.
[19] Kumar S, Dhiman SS. Exploring cone-shaped solitons, breather, and lump-forms solutions using the Lie symmetry method and unified approach to a coupled Breaking soliton model. Phys Scr. 2024;99:025243.
[20] Niwas M, Kumar S, Rajput R, Chadha D. Exploring localized waves and different dynamics of solitons in (2 + 1)-dimensional Hirota bilinear equation: a multivariate generalized exponential rational integral function approach. Nonlinear Dyn. 2024;112:9431–44.
[21] Kumar S, Hamid I. New interactions between various soliton solutions, including bell, kink, and multiple soliton profiles, for the (2+1)-dimensional nonlinear electrical transmission line equation. Opt Quant Electron 2024;56:1173.
[22] Baber MZ, Mohammed WW, Ahmed N, Iqbal MS. Exact solitary wave propagations for the stochastic Burgers' equation under the influence of white noise and its comparison with computational scheme. Sci Rep. 2024;14:10629.
[23] Ahmed AI, Algolam MS, Cesarano C, Rizk D, Gassem F. Dynamical behavior of the fractional generalized nonlinear Schrödinger equation of third-order. Opt Quantum Electron. 2024;56:843.
[24] Albosaily S, Elsayed EM, Albalwi MD, Alesemi M, Mohammed WW. The analytical stochastic solutions for the stochastic potential Yu-Toda-Sasa-Fukuyama equation with conformable derivative using different methods. Fractal Fract. 2023;7:787.
[25] Hamza AE, Alshammari M, Atta D. Fractional-stochastic shallow water equations and its analytical solutions. Results Phys. 2023;53:106953.
[26] Kundu A, Mukherjee A. Novel integrable higher-dimensional nonlinear Schrödinger equation: properties, solutions, applications. 2013. arXiv:1305.4023v1 [nlinSI].
[27] Kundu A, Mukherjee A, Naskar T. Modelling rogue waves through exact dynamical lump soliton controlled by ocean currents. Proc Roy Soc A-Math Phy. 2014;470:20130576.

[28] Mukherjee A, Kundu A. Novel nonlinear wave equation: Regulated rogue waves and accelerated soliton solutions. Phys Lett A. 2019;383(10):985–90.

[29] Mukherjee A, Janaki M, Kundu A. A new (2+1) dimensional integrable evolution equation for an ion acoustic wave in a magnetized plasma. Phys Plasmas. 2015;22(7):072302.

[30] Mohammed WW, Cesarano C, El-Morshedy M. The optical solutions of the stochastic fractional Kundu-Mukherjee-Naskar model by two different methods. Mathematics. 2022;10:1465.

[31] Biswas A, Vega-Guzman J, Bansal A, Kara AH, Alzahrani AK, Zhou Q, et al. Optical dromions, domain walls and conservation laws with Kundu-Mukherjee-Naskar equation via traveling waves and Lie symmetry. Results Phys. 2020;16:102850.

[32] Kudryashov NA. General solution of traveling wave reduction for the Kundu-Mukherjee-Naskar model. Optik. 2019;186:22–7.

[33] Ekici M, Sonmezoglu A, Biswas A, Belic MR. Optical solitons in (2+1)-Dimensions with Kundu-Mukherjee-Naskar equation by extended trial function scheme. Chinese J Phys. 2019;57:72–7.

[34] Yıldırım Y. Optical solitons to Kundu-Mukherjee-Naskar model with modified simple equation approach. Optik. 2019;184:247–52.

[35] Yıldırım Y. Optical solitons to Kundu-Mukherjee-Naskar model with trial equation approach. Optik. 2019;183:1061–5.

[36] Riesz M. L'intégrale de Riemann–Liouville et le probl ème de Cauchy pour l'équation des ondes. Bull Soc Math Fr. 1939;67:153–70.

[37] Wang KL, Liu SY. He's fractional derivative and its application for fractional Fornberg-Whitham equation. Therm Sci. 2016;1:54–54.

[38] Miller S, Ross B. An introduction to the fractional calculus and fractional differential equations. New York, NY, USA: Wiley; 1993.

[39] Caputo M, Fabrizio M. A new definition of fractional differential without singular kernel. Prog Fract Differ Appl. 2015;1(2):1–13.

[40] Sousa JV, de Oliveira EC. A new truncated fractional derivative type unifying some fractional derivative types with classical properties. Int J Anal Appl. 2018;16:83–96.

[41] Peng YZ. Exact solutions for some nonlinear partial differential equations. Phys Lett A. 2013;314:401–8.